JOURNAL OF GEOPHYSICAL RESEARCH, VOL. 106, NO. A3, PAGES 3603–3614. MARCH 1, 2001

Auroral polar cap boundary ion conic outflow observed on FAST

Y.-K. Tung,[1] C. W. Carlson,[1] J. P. McFadden,[1] D. M. Klumpar,[2]
G. K. Parks,[3] W. J. Peria,[3] and K. Liou[4]

Abstract. We observe large ion outflow fluxes ($> 10^8$ cm^{-2}s^{-1} mapped to 100 km) flowing from the auroral polar cap boundary on many FAST auroral passes near midnight. The outflow is in the form of ion conics composed mostly of light ions with energies of hundreds of eV. A statistical study of 606 FAST orbits during January and February 1997 was done to determine the MLT distribution and ion outflow properties relative to substorms. We find that the ion conic events occur most frequently near midnight, and therefore their direct magnetic connection to the nightside central plasma sheet makes this ion outflow a candidate for the ionospheric source of the nightside plasma sheet. To study the relationship between the ion conic outflow events and auroral substorm conditions, we use global auroral images acquired from the ultraviolet imager (UVI) on Polar. We find that the outflow events are well correlated with substorm expansion phase, but ion conic outflow events also occur during generally active aurora, when onset and expansion phases were not clearly identifiable. By combining FAST data to determine ion outflow fluxes and ILAT extent and Polar UVI images to determine MLT extent, we estimate the total outflow due to these ion conic events to be 10^{22} to 10^{24} ions/s. By comparing with earlier ion outflow studies, we conclude that these polar cap boundary ion conic events are not the dominant or only ionospheric source of ion outflow over the entire auroral oval but are the dominant nightside auroral ion outflow.

1. Introduction

The relative importance of the ionosphere versus the solar wind as a source of ions for the plasma sheet has long been an unresolved issue in space physics. In recent years, some have suggested that the ionosphere is an important, if not dominant, ion source for the plasma sheet and ring current [*Chappell et al.*, 1987]. In this paper, we present observations of an ionospheric ion source in the form of an ion conic observed near the poleward edge of the nightside aurora. On FAST, the ion outflow associated with the ion conic near the polar cap boundary accounts for most of the total nightside auroral ion outflow on many auroral passes.

Ion conics were first observed by *Sharp et al.* [1977] from the satellite 1976-65B as ion distributions with peaks at the pitch angles 30°-140° and a minimum along the magnetic field direction. Using S3-3 data, *Gorney et al.* [1981] characterized the occurrence properties of ion conics and upward ion beams. The first quantitative study of auroral and polar cap ion outflow sources was done by *Yau et al.* [1985] using DE-1 data. In their study, the noon sector is the dominant source of ionospheric ions; though during active times ($K_p > 3$), the nightside outflow is enhanced to almost comparable levels. Subsequent work has involved statistically characterizing the shape of the ion conic distribution [*Peterson et al.*, 1992], altitude dependence of heating [*Miyake et al.*, 1993, 1996], altitude, MLT, and ILAT occurrence frequencies of ion conics and beams on DE-1 [*Kondo et al.*, 1990], altitude, MLT, and ILAT occurrence frequencies of ion conics and beams on Viking [*Thelin et al.*, 1990], and the occurrence frequency of types of ion conics (defined by association with wave activity and MLT location) [*André et al.*, 1998]. Recent reviews [*Yau and André*, 1997; *André and Yau*, 1997; *Chang and André*, 1998; *Shelley*, 1995] provide more detail on the ion outflow work.

As one of the results of *Yau et al.* [1985] was that the cusp/cleft is the major source of ionospheric ions, dayside outflow studies have been done by *Lockwood et al.* [1985a, b] and *Moore et al.* [1996], and modeling has been done of the convection electric field to trace

[1]Space Sciences Lab, University of California, Berkeley.
[2]Lockheed Martin Palo Alto Research Labs, Palo Alto, California.
[3]Geophysics Program, University of Washington, Seattle.
[4]Applied Physics Lab, Johns Hopkins University, Laurel, Maryland.

Paper number 2000JA900115.
0148-0227/01/2000JA900115$09.00

the ion outflow from the dayside to the nightside plasma sheet [*Lockwood et al.*, 1985b]. On the nightside, though studies have concentrated on ion conic and beam distribution and occurrence frequencies, quantitative ion outflow studies have not been done in recent years.

The nightside polar cap region has become an area of recent interest [*Savaud et al.*, 1999; *Yamamoto et al.*, 1993] from the point of view of coordinated studies involving precipitating ions, electric field structures, and auroral images. We complement this work by providing a statistical study of the ion outflow in this region due to ion conics. The nightside polar cap boundary ion conics we observe on FAST are located on magnetic field lines directly connected to the nightside plasma sheet. Therefore unlike ions from the cleft ion fountain, the ions outflowing from these nightside events do not rely on convection to carry them over the polar cap into the central plasma sheet. On the basis of Polar Ultraviolet Imager (UVI) images, we find that the flow is associated with substorm expansion phase in many well-defined substorms. However, we also find that ion outflow also occurs during generally active aurora without any clear substorm structure.

This paper describes a statistical study undertaken to quantify where these ion conic events occur and how the outflow varies as a function of substorm phase, and to estimate the total ions/s that this outflow contributes to the magnetosphere. We proceed by describing the instrumentation, showing features of a typical event, describing the procedure used to compile the statistics, and presenting our results. We find that the ion conic events tend to occur near local magnetic midnight and are associated with substorm expansion phase though not exclusively and that the total outflow is in the 10^{22}-10^{24} ions s^{-1} range.

2. Instrument Description

The FAST satellite was launched in August 1996 and has an elliptical polar 4180 × 350 km orbit with an inclination of 83°. It has a full complement of three-dimensional particle detectors and wave instruments [*Carlson et al.*, 1998]. In this study, we examine data from the electron electrostatic analyzers (EESA) and ion electrostatic analyzers (IESA) that measure full pitch angle distributions in the sweep time of the detector (78 ms). In addition, we use data from the Time-of-Flight Energy And Mass Spectrometer (TEAMS), which is an ion electrostatic analyzer followed by a time-of-flight section to separate masses.

In this study, we use summary data from the FAST campaign period of January and February 1997, when the spacecraft was in a noon-midnight orbital plane with apogee over the Northern Hemsiphere. The time resolution of the summary data is the spin period of 5 s. Ion composition is obtained from the TEAMS instrument summary data. We use the east-west component of the three-axis fluxgate magnetometer to determine the sense of the field-aligned current (up/down).

The Polar spacecraft was launched on February 24, 1996, into a highly elliptical, Sun-inertial orbit with an apogee of 9 R_E geocentric over the Northern Hemisphere. The UVI on board the Polar spacecraft is mounted on a despun platform, allowing continuous monitoring of the Northern Hemispheric auroral oval for 12 hours out of the 18-hour orbit period. There are five filters operated on UVI to measure airglow emissions in five FUV bands. In the present study, we use auroral images taken with the two major filters in the Lyman-Birge-Hopfield bands centered at 150 and 170 nm. See *Torr et al.* [1995] for a detailed description of the UVI instrument.

3. Event Overview

In Plate 1, we present a polar cap boundary ion conic event from orbit 1809, a typical FAST nightside auroral crossing during January and February 1997. The top four panels show electron and ion ESA pitch angle and energy spectrogram data. Panels 5 and 6 are data from the TEAMS instrument that show H^+ and O^+ fluxes, respectively. The seventh panel shows ion number flux for energies greater than 20 eV integrated over all pitch angles of the IESA, while panel 8 shows the cumulative number flux over the auroral pass (the integral of the curve in panel 7). Panel 9 shows the ion energy flux for energies greater than 20 eV integrated over all pitch angles of the IESA. Both number and energy fluxes have been mapped to 100 km altitude, so that the data from different passes with varying altitudes can be compared directly. The east-west component (z-component) of the magnetometer data is shown in panel 10; positive slope indicates a downward current.

The polar cap boundary ion conic is located from 1725:40 to 1726:40 UT, adjacent to the polar cap boundary of the aurora. It is characterized by intense ion fluxes, evident both in the large energy fluxes seen at energies from 10 to several hundred eV in panels 3 and 4 and in the high outflow number flux in panel 7. Note that panel 7 has a logarithmic vertical scale, so that the outflow is an order of magnitude higher during the ion conic than anywhere else in the pass. We wish to point out that the integral of the number flux includes the high energy precipitating ion population, and therefore the curve in panel 7 represents an underestimate of the ion conic outflow flux. However, the high energy ion population is largely isotropic (except for the loss cone) and therefore contributes relatively little when integrated over all pitch angles. A few case studies reveal that the contribution is of the order of a few percent. The cumulative ion outflow shown in panel 8 shows that the dominant contribution to the total auroral outflow is from the polar cap boundary ion conic. The reader is cautioned that because the integral in panel 8 has not been adjusted for spacecraft trajectory angle, its units are not physically meaningful. Rather, it should simply be interpreted as a means of demonstrating that a large fraction of the ion outflow occurs adjacent to the

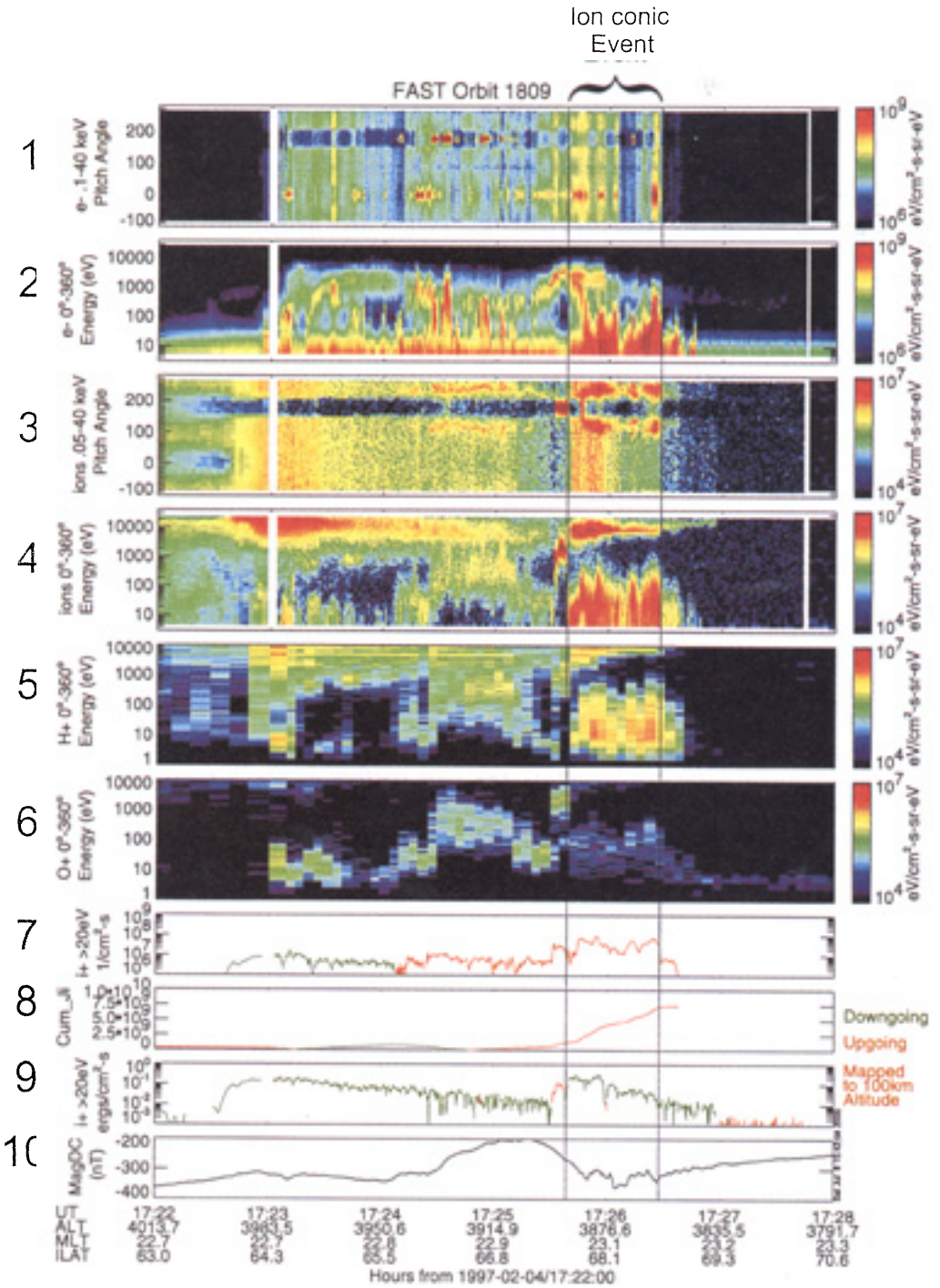

Plate 1. A typical FAST nightside auroral pass showing the ion conic at the polar cap boundary of the aurora. Panels 1 and 2 show electron ESA pitch angle and energy plots, while panels 3 and 4 show ion ESA pitch angle and energy plots. The ion conic occurs from 1725:40 to 1726:40 UT and can be seen as intense fluxes at 130° and 230° pitch angle in panel 3. As seen in panel 4, the energy ranges from a few eV to a few hundred eV. Simultaneous with the ion conic are highly structured filamentary regions of upward and downward electrons, apparent from panels 1 and 2. Panels 5 and 6 are H^+ and O^+ data from the TEAMS instrument that show the predominance of H^+ over O^+ at the polar cap boundary. Panel 7 shows integrated IESA number flux for all pitch angles above 20 eV energy. A net downward flux is shown in green, while a net upward flux is in red. Panel 8 is the integral of panel 7. Notice that the outflow at the polar cap dominates this integral. Panel 9 shows the integrated IESA energy flux for all pitch angles above 20 eV energy. Panel 10 shows the east-west magnetic field component, where a positive slope indicates a downward current.

polar cap boundary. Coincident with the ion conic are highly structured, filamentary regions of upward and downward electron beams, apparent in this case from the intense fluxes at 10 to hundreds of eV in panel 2 and enhancements in flux at 0° and 180° pitch angle in panel 1. Though not seen in this orbit, there is often a counterstreaming electron population associated with the polar cap boundary ion conic as well.

From panels 5 and 6, we can see that the outflow is predominantly hydrogen, with a small amount of oxygen. Panel 10 shows that the field-aligned current structure during the ion conic is filamentary, with many small regions of upward and downward current. Last, we note that dispersed high-energy ions visible in panel 4, the ion energy spectrogram, are often observed at the same time as the polar cap boundary ion conic.

4. Statistical Study

Statistical studies were done to quantify the conditions under which ion conic events were observed and to characterize the outflow properties. Specifically, we examined the MLT location of the events and their occurrence relative to substorm onset times.

4.1. Identifying Events

Since the goal of the study was to characterize ion conic outflow near the auroral polar cap boundary, the FAST IESA summary data were screened by eye, and ion conic events were identified using two criteria: (1) they occurred immediately adjacent to the polar cap boundary (as identified by IESA data), and (2) the integrated ion outflow over all pitch angles and over energies greater than 20 eV exceeded 10^8 cm^{-2} s^{-1} for at least one 5-s average (when mapped to 100 km altitude).

In order to normalize the data, we identified nonevents as well. A nonevent was defined as a FAST nightside polar cap boundary crossing where the 5-s average ion outflow flux never exceeded 10^8 cm^{-2} s^{-1}.

Though deciding between events and nonevents and start and end times of polar cap boundary ion conic events were determined by eye, all subsequent analysis and calculations were not subject to potentially subjective factors such as color scale and plot ranges. Indeed, whether a particular ion conic event met criteria 2 above, though initially determined by eye, was verified after initial selection by comparing outflow values against the threshold of 10^8 cm^{-2} s^{-1}.

Orbits during January and February 1997, the FAST campaign period, were selected because of the noon-midnight orientation of the orbital plane, and the events were observed to occur near the midnight sector. Though a comprehensive search was not performed, examination of many orbits in the dawn-dusk orientation did not reveal any polar cap boundary ion conic outflow events.

4.2. Results

Figure 1 is a histogram showing the distribution of ion outflow events in magnetic local time. The plot is normalized so that the y axis shows frequency of occurrence. The events occur near local magnetic midnight, where the magnetic field lines connect directly to the nightside plasma sheet. A mapping using the Tsyganenko 89 magnetic field model [*Tsyganenko*, 1989]

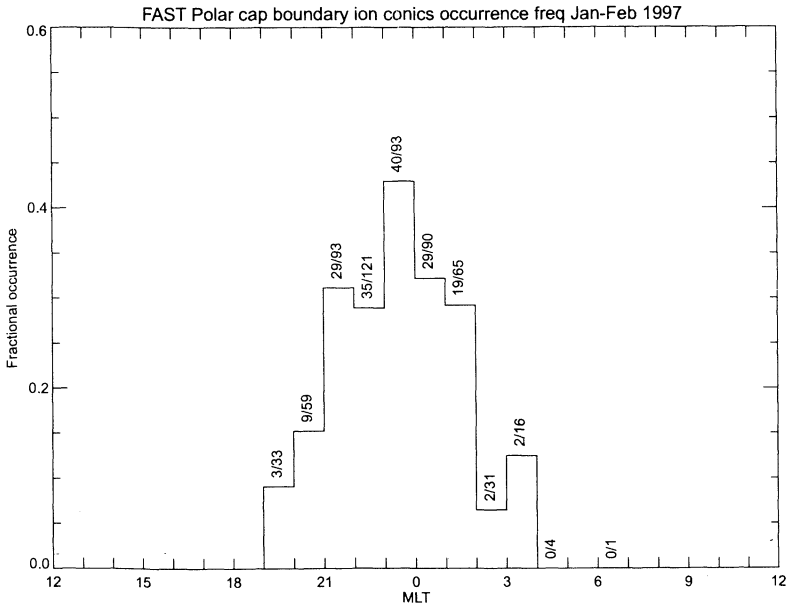

Figure 1. A histogram showing the MLT distribution of the ion conic events. Data have been normalized to account for uneven distribution of FAST orbits in MLT sectors. The number of events and the total number of FAST auroral crossings in each MLT sector is listed above each histogram bin of 1 hour MLT.

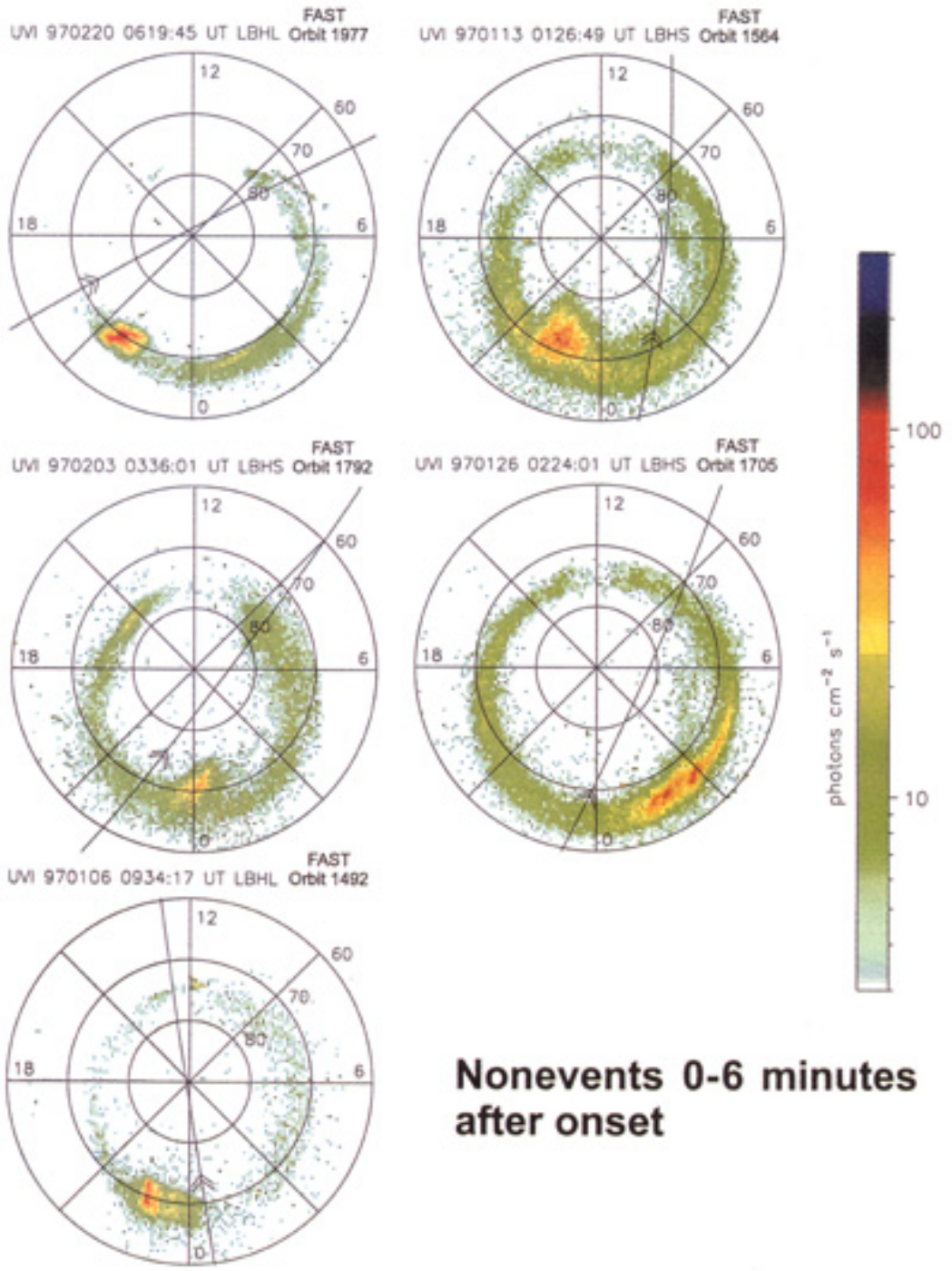

Plate 2. Polar UVI images with FAST orbit trajectory and location overlaid. These five images are for FAST orbits when ion conic outflow events were not observed. Each of these polar cap boundary crossings occurs 0-6 min after a substorm onset.

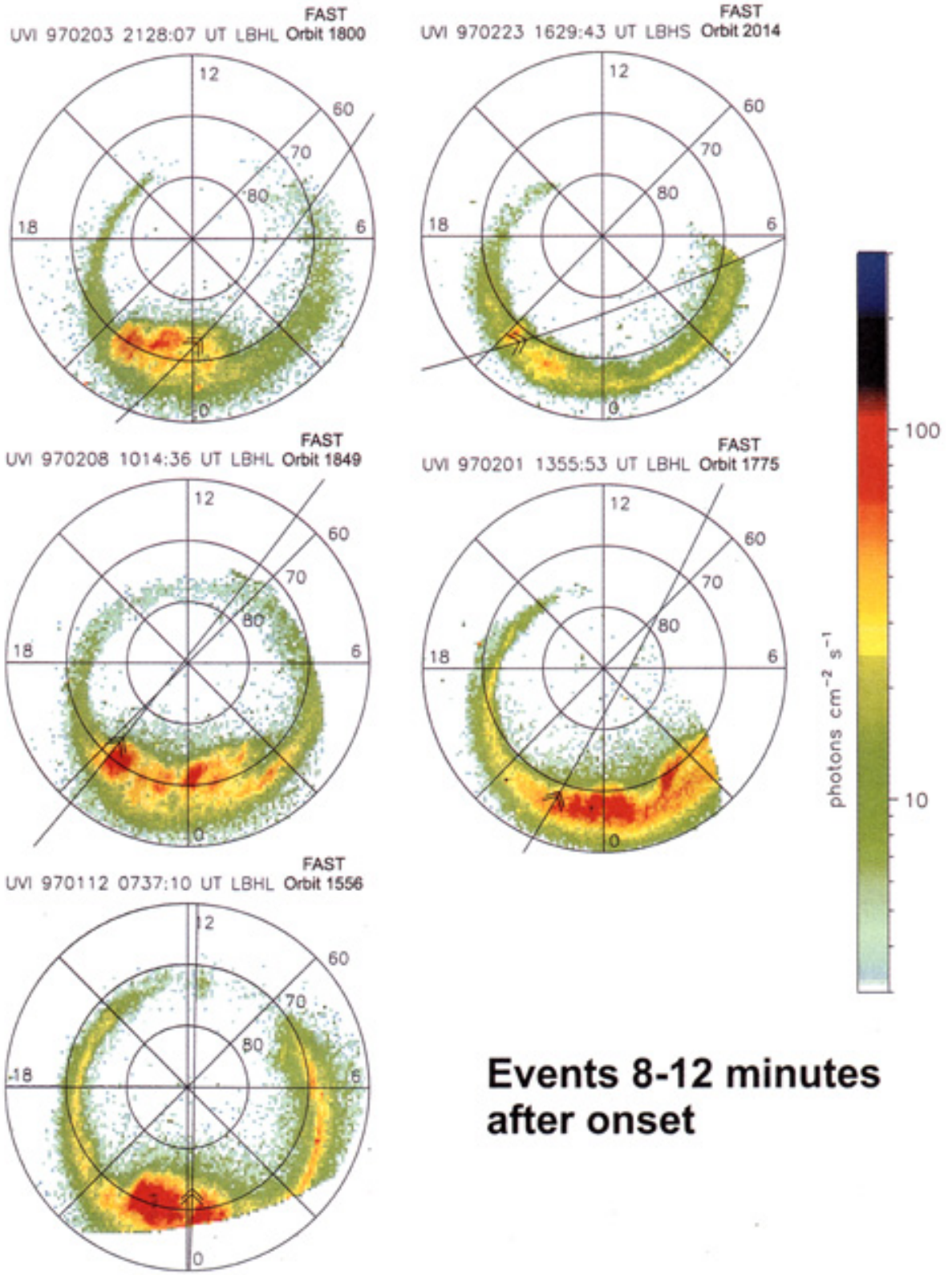

Plate 3. Same as Plate 2, but for FAST orbits in which ion outflow events are observed. Each of these ion conic outflow events occurs 8-12 min after a substorm onset.

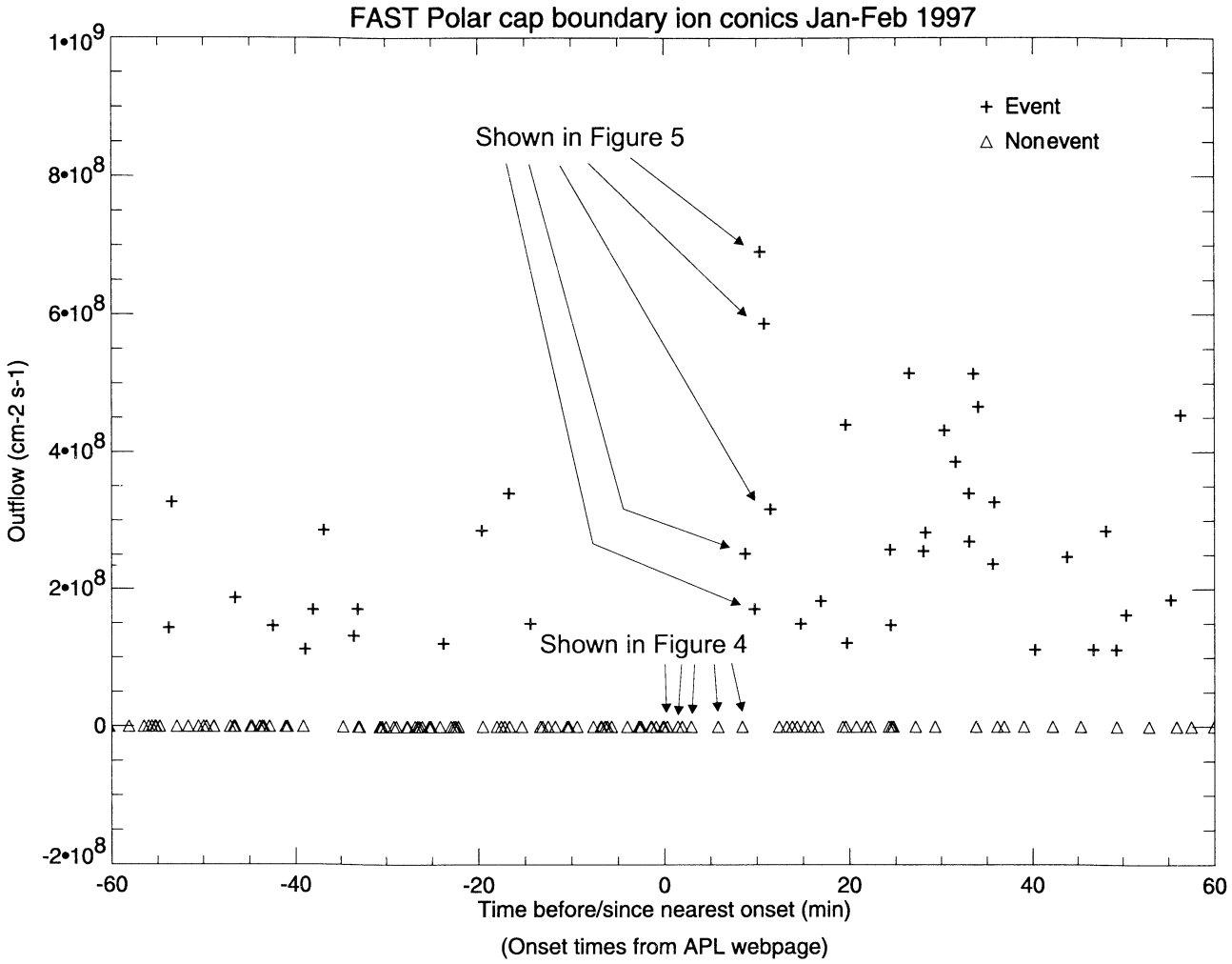

Figure 2. Plot of outflow flux versus time since/before substorm onset. Ion conic events are denoted by a cross, while nonevents (FAST auroral crossings) are plotted as a triangle at 0 outflow.

shows that the ion conic occurs on L shells ranging from 22 to 31 R_E. This result is corroborated by the frequent coincidence of polar cap boundary ion conics with high energy dispersed ions, which we interpret as a signature that the polar cap boundary ion conic is magnetically connected to the nightside reconnection X line.

Substorm onset times were obtained from the Auroral Particle and Imagery Group at the Johns Hopkins University Applied Physics Lab webpage (http://sd-www.jhuapl.edu/Aurora/polar_movies/UVI_polar_movies.html). Onset times were identified when Polar UVI images showed both an auroral brightening ("breakup") and a clear expansion phase. A delay time and a prior time were calculated for every ion conic event, and the times are plotted versus peak ion outflow in Figure 2. The peak ion number flux during the event is used as an indicator of the strength of the event because, unlike the average outflow or integrated outflow over the event, it is not sensitive to the specific start and end times. Note that the substorm onset time list contains only those times when a clear onset and expansion phase was observed in the UVI data. There are periods of generally active aurora for which no clear onset time was identified. Therefore there are ion conic events in the database occurring up to 4000 min after onset, but the large delay times are due to long periods of time without identified substorm onsets rather than to physically meaningful conditions. Because substorms generally last no more than 30-60 min, points beyond 60 min are not plotted. Though not shown, the portion of events selected in Figure 2 have a similar MLT distribution to Figure 1.

In Figure 2, note that generally higher outflow occurs after substorm onset than before. In addition, the proportion of events (versus nonevents) is higher after substorm onset. In the 60 min before onset, there were 13 events and 79 nonevents, an occurrence rate of 14%. In the 60 min after onset, however, there are 30 events and 36 nonevents, an occurrence rate of 45%. The average outflow of events before onset is 1.98×10^8 $cm^{-2}s^{-1}$,

while the average outflow of events after onset is 3.01×10^8 cm^{-2}s^{-1}. These results are consistent with the picture that ion conic outflow events are associated with substorm expansion phase. In addition, we speculate that the higher density of events around 30 min after onset is due to the fact that the enhancement in the aurora has grown in MLT extent, so that FAST has a higher chance of passing through it. The growth in MLT extent means a larger outflow occurs at this time.

A closer study of Polar UVI images was done for specific events (and nonevents) near substorm onsets, and we find that nonevents that occur immediately after onset are due to FAST being in the wrong MLT location. We examined a time series of sequential images over a 10-min interval centered on the FAST polar cap crossing time for each event and nonevent. To connect the Polar UVI images to FAST, the UVI image and the FAST trajectory (and location) are overplotted in ILAT/MLT coordinates. Since the Polar UVI image is integrated over 18 or 36 s, the FAST position and direction of travel are indicated by two arrows, one representing the position at the beginning of the image and another representing the position at the end of the image. Plate 2 shows a series of representative Polar UVI images for the nonevents that occur 0-6 min after substorm onset. Note that in all these images, the FAST orbit does not pass through the brightened spot that is the substorm onset. In contrast, Plate 3 shows a series of representative Polar UVI images for the events that occur 8-12 min after onset. In all of these cases, the FAST orbit passes directly through the brightened auroral onset spot. Though the correlation is clear near substorm onset, it is not so clear, however, for events that are not close to substorm onsets. One reason is that the auroral structure is not so clear; there is no clear spot to speak of. Another reason is that perhaps

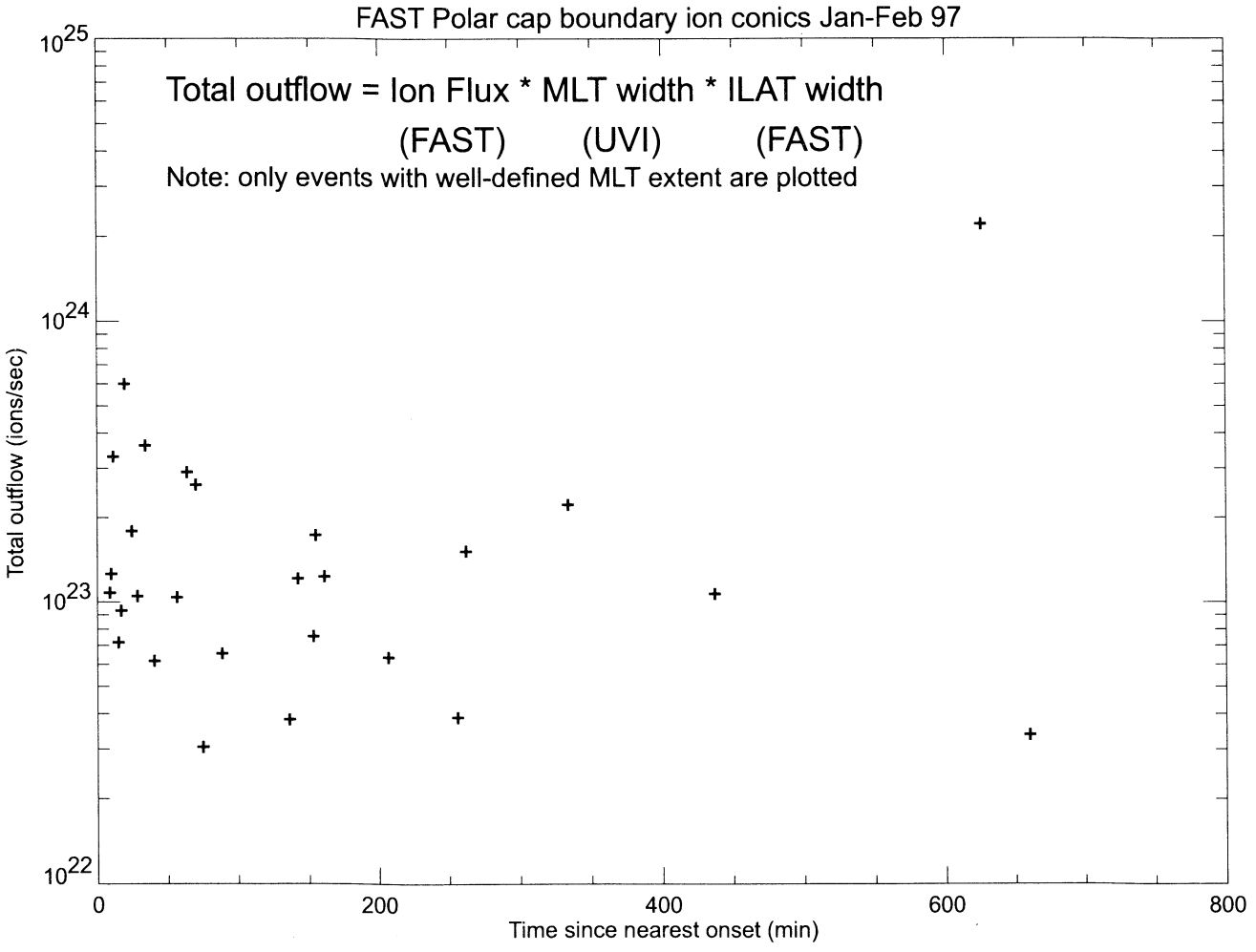

Figure 3. Total outflow of ion conics plotted versus time since nearest substorm onset. The total outflow is calculated by taking ion flux (over all pitch angles and energies > 20 eV) as measured by FAST and multiplying by the area over which the flux is observed. The ILAT extent is determined by FAST, while the MLT extent is estimated from Polar UVI images. Only the 27 events for which MLT extent could be estimated are plotted.

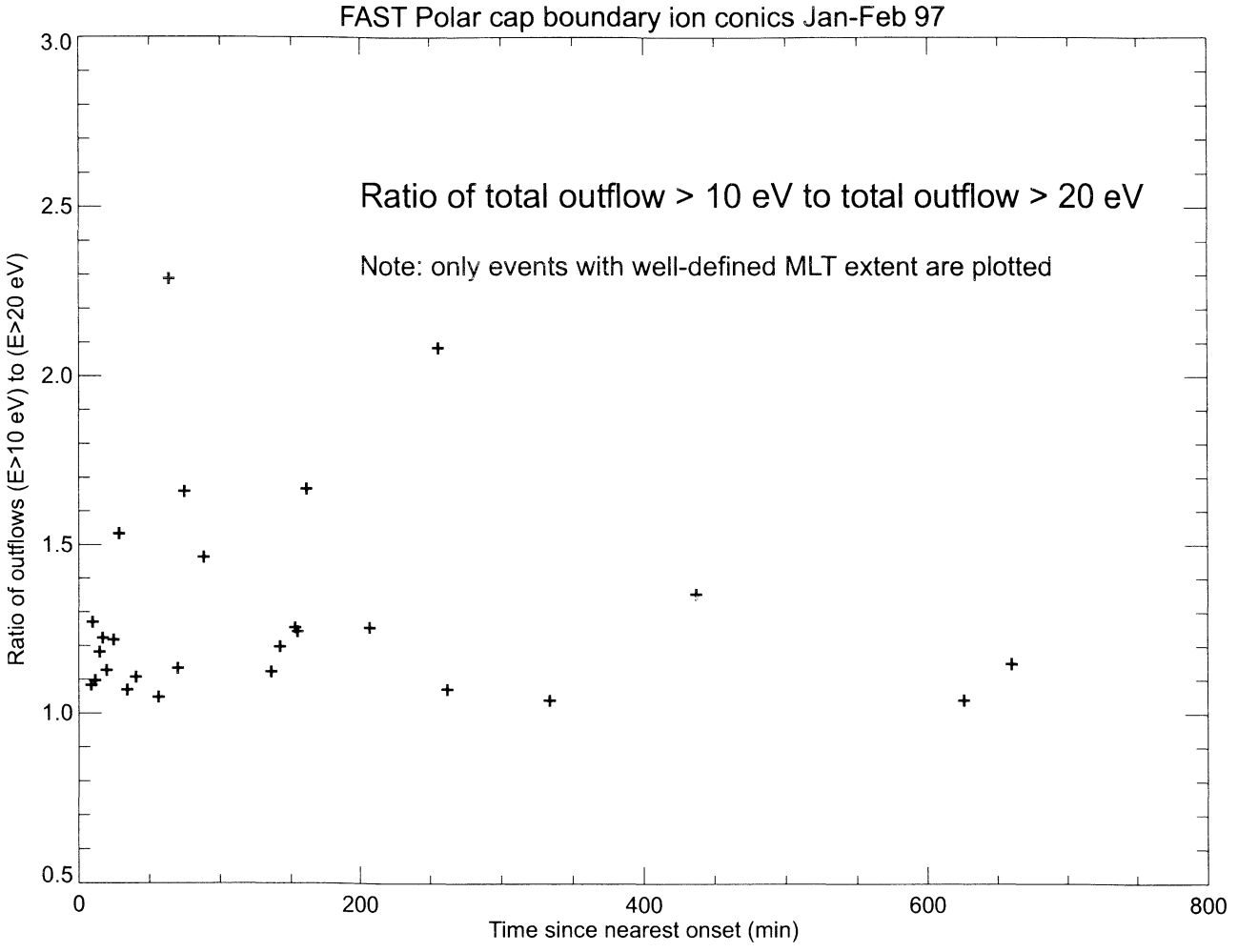

Figure 4. Ratio of total outflow > 10 eV to total outflow > 20 eV plotted versus time since nearest substorm onset. The plot shows how much additional flux particles between 10 and 20 eV contribute.

these ion conic events are associated with generally active aurora with onsets and expansions being just one example of active aurora.

4.3. Total Outflow

In order to understand the importance of the contribution to the total ion outflow of these polar cap boundary ion conics, we estimate quantitatively the total ion outflow due to these ion conics by multiplying observed fluxes by the area over which ion outflow is observed. The area can be approximated as a rectangle with a MLT extent and an ILAT extent.

The outflow flux level and the ILAT extent of the ion conics is obtained from FAST data. The conic ILAT extent is determined from FAST summary energy fluxes. However, the MLT extent is more difficult to estimate. By examining over 400 sets of UVI images during times of FAST auroral crossings, we concluded that we could estimate the MLT extent of ion outflow in certain cases. Near spot-like onset times, the ion outflow was confined to the location of the UV emissions. A MLT extent was estimated based on the size of the UV spot in 27 cases. The small number of cases for which this was done reflects the difficulty of the task and represents our best judgment based on examination of multiple FAST orbit crossings of "near misses" and "near hits." We note that the estimate of the size of the spot was done by eye using a false-color image, and therefore the MLT extent should be regarded as having an uncertainty of approximately a factor of 2. The UVI images used in this study were not adjusted for the wobble of the despun platform, but we note that the 10 pixel smearing due to the wobble in the worst case when the wobble is in the latitudinal direction accounts for less than 1 MLT in width at a typical auroral polar cap boundary latitude of 70°. In addition, there were many instances of generally active aurora in which it was difficult to estimate the MLT extent of outflow, and so we concentrate

on the subset of events for which we could estimate the MLT extent of the outflow.

Figure 3 shows a plot of the 27 events for which MLT extent could be estimated, with outflow versus time since substorm onset plotted. The average MLT extent for these 27 events is 1.89 hours, with values ranging from 1 to 4 hours of MLT. Note that most of the outflows are in the range 10^{23} ions s^{-1} with one event in the 10^{24} ions s^{-1} range.

The ion outflow flux used is an integral of the number flux over all pitch angles for energies greater than 20 eV (The energy was chosen high enough so as to avoid the majority of spacecraft charging effects on FAST). Because this excludes all fluxes with energies less than 20 eV, the total outflow is an underestimate. We show in the discussion below that this underestimate does not significantly change our results.

In order to estimate the amount of outflow contributed by low energy ions, the integral of total outflow was done for all energies above 10 eV and for all energies above 4.6 eV, which is the lowest energy channel. Note that all these energies are relative to the spacecraft potential, which is generally a few volts positive during these events. The ratio of the outflow above 10 eV to the outflow above 20 eV generally falls in the range between 1 and 2 and is shown in Figure 4. The ratio of the outflow above 4.6 eV to the outflow above 20 eV is higher, with a handful of events in the range between 2 and 3, but the majority of the events have a ratio between 1 and 2 (shown in Figure 5). This suggests that the low energy ion spectrum is rather flat and that adding the contribution of ions with energy less than the spacecraft potential would not affect the total outflow result by much more than a factor of 2, which is the approximate uncertainty of the result.

In order to see if these 27 events exhibited outflow values typical of the 168 events we have observed, we calculated the total outflow associated with each of the

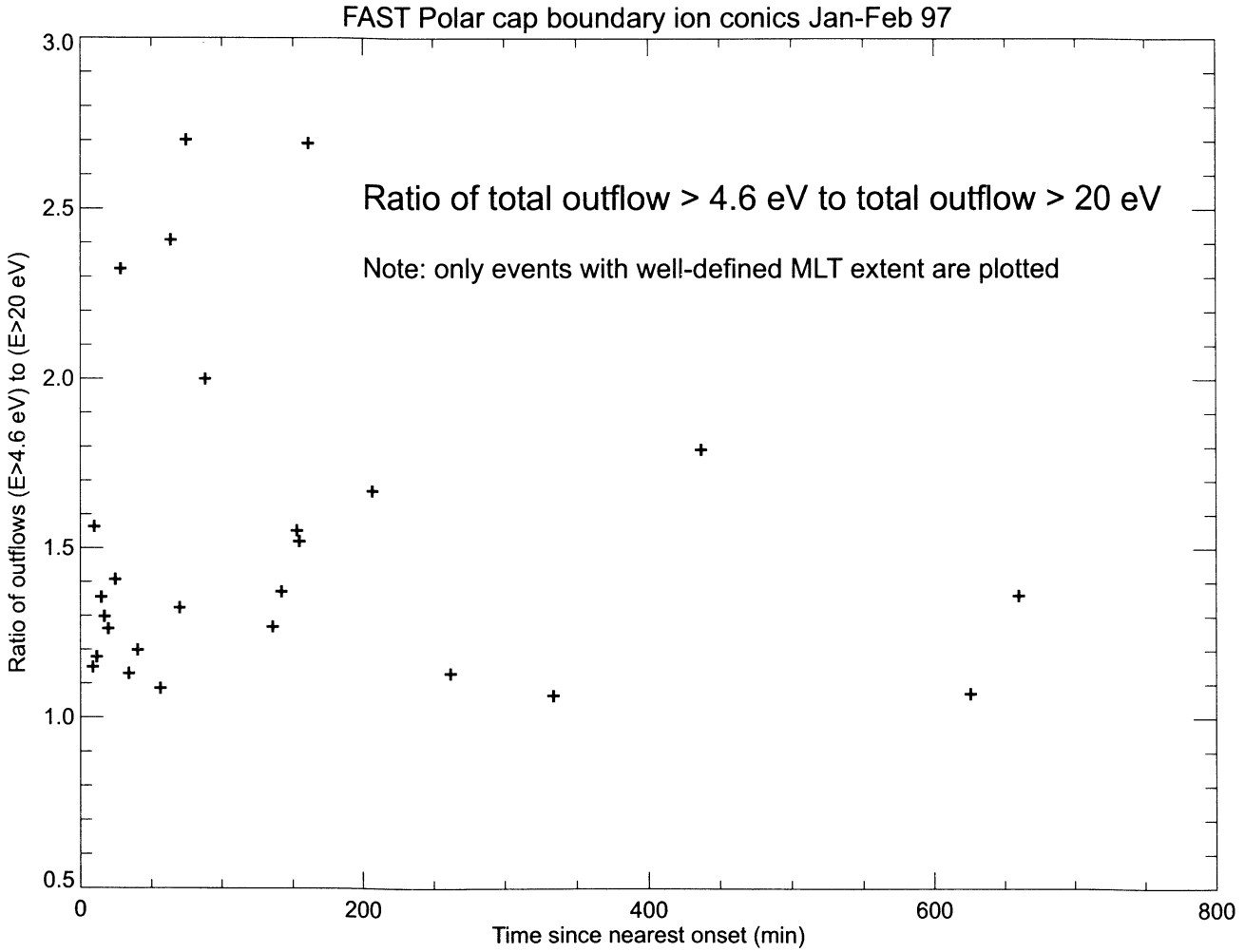

Figure 5. Ratio of total outflow > 4.6 eV to total outflow > 20 eV plotted versus time since nearest substorm onset. The plot shows how much additional flux particles between 4.6 and 20 eV contribute.

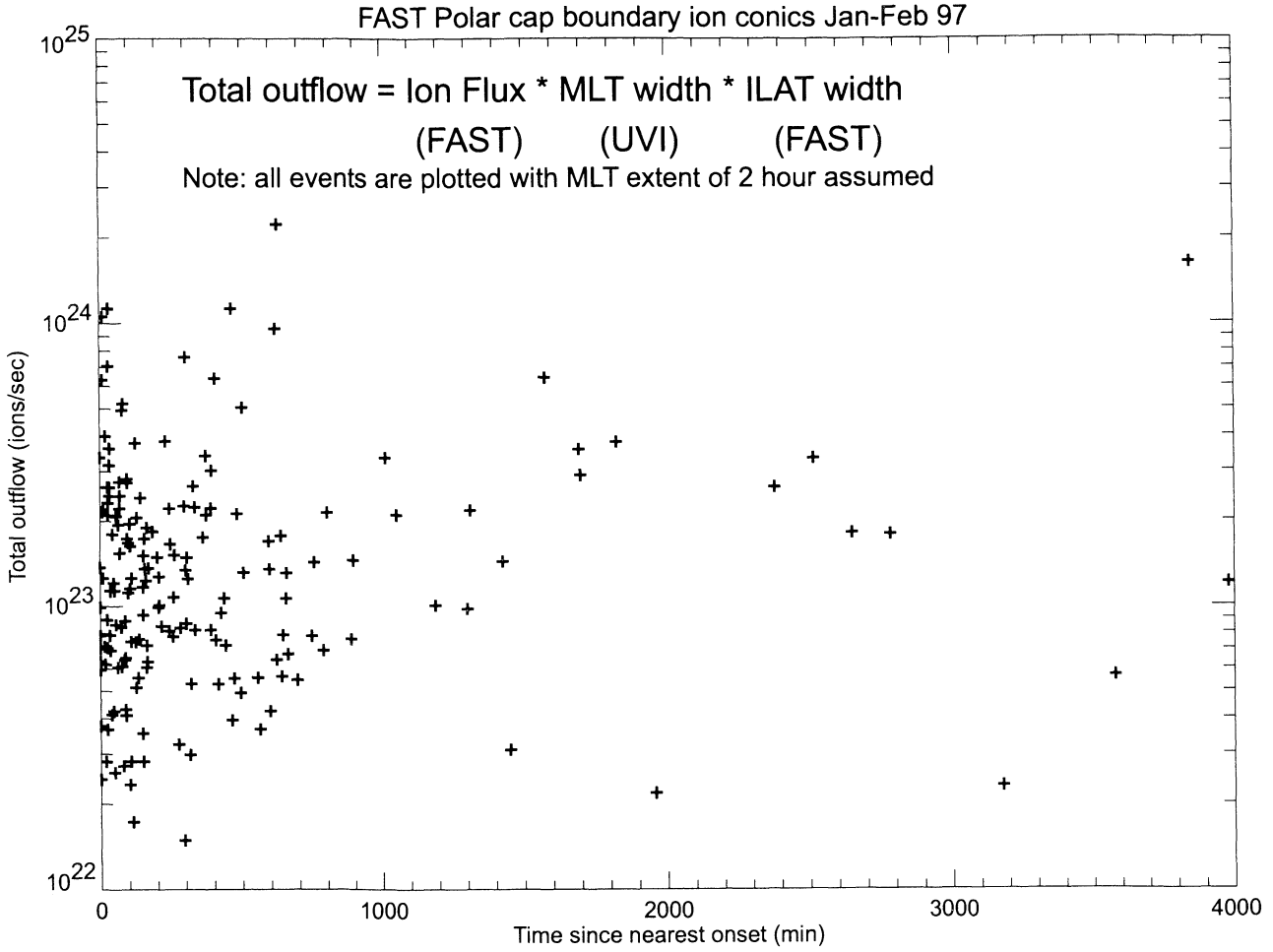

Figure 6. Total outflow of all ion conic events plotted versus time since nearest substorm onset. Since many of these events did not have a clear MLT extent as identified by Polar UVI images, a nominal width of 2 MLT has been used in the total outflow calculation.

168 events, assuming a 2 hour MLT extent. The result is shown in Figure 6. The outflow is in the same range (10^{22} to 10^{24} s^{-1}) as the 27 events with well-defined MLT extent, suggesting that the 27 events are representative in terms of total outflow.

Our outflow values are small compared to total auroral outflow values reported by *Yau et al.* [1985], which are in the 10^{25} ions/sec range, suggesting that the polar cap boundary ion conics reported here do not constitute the majority of auroral ion outflow. However, the observed fluxes of the ion conics ($> 10^8$ cm^{-2} s^{-1}) are generally higher than those reported by *Yau et al.* [1985] in the 21-03 MLT sector, suggesting that the polar cap boundary ion conics are the dominant ion outflow in the nightside sector.

5. Conclusions

Polar cap boundary ion conics are prevalent in the FAST data and are a major source of near-midnight outflow from the ionosphere, as they often dominate the total ion outflow of the entire nightside auroral pass. By observing UVI data, we find that near well-defined substorm onsets, the polar cap boundary auroral ion outflows are correlated with substorm expansion phase. However, ion outflow events also occur during generally active aurora when no clear substorm structure is apparent in the UVI data. We calculate the total outflow due to these events to be 10^{22} to 10^{24} ions s^{-1} and conclude, based on comparison with *Yau et al.* [1985] results, that nightside polar cap boundary ion conic outflow is not the dominant ionospheric source of ions over the entire oval but is the dominant nightside ion outflow. Their location on the nightside and therefore easy entry into the plasma sheet is a compelling reason for them to be a candidate for the ionospheric source of the plasma sheet population.

Acknowledgments. We would like to thank F.S. Mozer, W.K. Peterson, and E.J. Lund for helpful comments.

This work was supported by NASA under grants NGT5-50061 and NAG5-3596.

Hiroshi Matsumoto thanks D. Schriver and T. Mukai for their assistance in evaluating this paper.

References

André, M., and A. Yau, Theories and observations of ion energization and outflow in the high latitude magnetosphere, *Space Sci. Rev., 80,* 27-48, 1997.

André, M., P. Norqvist, L. Andersson, L. Eliasson, A.I. Eriksson, L. Blomberg, R.E. Erlandson, and J. Waldemark, Ion energization mechanisms at 1700 kilometer in the auroral region, *J. Geophys. Res., 103,* 4199-4222, 1998.

Carlson, C.W., R.F. Pfaff, and J.G. Watzin, The Fast Auroral SnapshoT (FAST) mission, *Geophys. Res. Lett., 25,* 2013-2016, 1998.

Chang, T., and M. André, Recent developments of ion acceleration in the auroral zone, in *Geospace Mass and Energy Flow, AGU Geophys. Monog. Ser.* vol. 104, edited by J.L. Horwitz, D.L. Gallagher, W.K. Peterson, pp. 115-128, AGU, Washington, D.C., 1998.

Chappell, C.R., T.E. Moore, and J.H. Waite Jr., The ionosphere as a fully adequate source of plasma for the Earth's magnetosphere, *J. Geophys. Res., 92,* 5896-5910, 1987.

Gorney, D.J., A. Clarke, D. Croley, J.F. Fennell, J. Luhmann, and P. Mizera, The distribution of ion beams and conics below 8000 km, *J. Geophys. Res., 86,* 83-89, 1981.

Kondo, T., B.A. Whalen, A.W. Yau, and W.K. Peterson, Statistical analysis of upflowing ion beam and conic distributions at DE-1 altitudes, *J. Geophys. Res., 95,* 12,091-12,102, 1990.

Lockwood, M., M.O. Chandler, J.L. Horwitz, J.H. Waite, Jr., T.E. Moore, and C.R. Chappell, The cleft ion fountain, *J. Geophys. Res., 90,* 9736-9748, 1985a.

Lockwood, M., J.H. Waite Jr., T.E. Moore, J.F.E. Johnson, C.R. Chappell, A new source of suprathermal O+ ions near the dayside polar cap boundary, *J. Geophys. Res., 90,* 4099-4116, 1985b.

Miyake, W., T. Mukai, and N. Kaya, On the evolution of ion conics along the field line from EXOS-D observations, *J. Geophys. Res., 98,* 11,127-11,134, 1993.

Miyake, W., T. Mukai, and N. Kaya, On the origins of the upward shift of elevated (bimodal) ion conics in velocity space, *J. Geophys. Res., 101,* 26,961-26,969, 1996.

Moore, T.E., C.J. Pollock, M.L. Adrian, P.M. Kintner, R.L. Arnoldy, K.A. Lynch, and J.A.Holtet, The cleft ion plasma environment at low solar activity, *Geophys. Res. Lett., 23,* 1877-1880, 1996.

Peterson, W.K., H.L. Collin, M.F. Doherty, and C.M. Bjorklund, O+ and He+ restricted and extended (bi-modal) ion conic distributions, *Geophys. Res. Lett., 9,* 1439-1442, 1992.

Savaud, J.-A., D. Popescu, D.C. Delcourt, G.K. Parks, M. Brittnacher, V. Sergeev, R.A. Kovrazhkin, T. Mukai, and S. Kokubun, Sporadic plasma sheet ion injections into the high-altitude auroral bulge: Satellite observations, *J. Geophys. Res., 104,* 28,565-28,586, 1999.

Sharp, R.D., R.G. Johnson, and E.G. Shelley, Observation of an ionospheric acceleration mechanism producing energetic (keV) ions primarily normal to the geomagnetic field direction, *J. Geophys. Res., 82,* 3324-3328, 1977.

Shelley, E.G., The auroral acceleration region: The world of beams, conics, cavitons, and other plasma exotica, U.S. Natl. Rep. Int. Union Geod. Geophys. 1991-1994, *Rev. Geophys., 33,* 709-714, 1995.

Thelin, B., B. Aparicio, and R. Lundin, Observations of upflowing ionospheric ions in the mid-altitude cusp/cleft region with the Viking Satellite, *J. Geophys. Res., 95,* 5931-5939, 1990.

Torr, M.R., et al., A far ultraviolet imager for the International Solar-Terrestrial physics mission, *Space Sci. Rev., 71,* 329-383, 1995.

Tsyganenko, N.A., A magnetospheric magnetic field model with the warped tail current sheet, *Planet. Space Sci., 37,* 5-20, 1989.

Yamamoto, T., E. Kaneda, H. Hayakawa, T. Mukai, A. Matsuoka, S. Machida, H. Fukunishi, N. Kaya, K. Tsuruda, and A. Nishida, Meridional structures of electric potentials relevant to premidnight discrete auroras: A case study from Akebono measurements, *J. Geophys. Res., 98,* 11,135-11,151, 1993.

Yau, A.W., and M. André, Sources of ion outflow in the high latitude ionosphere, *Space Sci. Rev., 80,* 1-25, 1997.

Yau, A.W., E.G. Shelley, W.K. Peterson, and L. Lenchyshyn, Energetic auroral and polar ion outflow at DE 1 altitudes: magnitude, composition, magnetic activity dependence, and long-term variations, *J. Geophys. Res., 90,* 8417-8432, 1985.

C. W. Carlson, J. P. McFadden, and Y.-K. Tung, Space Sciences Lab, University of California, Berkeley, CA 94720. (yktung@ssl.berkeley.edu)

D. M. Klumpar, Lockheed Martin Palo Alto Research Labs, 3251 Hanover St., Palo Alto, CA 94304.

K. Liou, Applied Physics Laboratory, Johns Hopkins University, Laurel, MD 20723.

G. K. Parks and W. J. Peria, Geophysics Program, University of Washington, Seattle, WA 98195.

(Received April 20, 2000; revised August 7, 2000; accepted August 7, 2000.)